

Magnetic excitations in the inelastic neutron scattering spectra of the intermediate-valence compounds $\text{Sm}(\text{M})\text{B}_6$ ($\text{M} = \text{Ca}, \text{Ba}, \text{La}$)

P. A. Alekseev, V. N. Lazukov, and I. P. Sadikov

Kurchatov Institute Russian Scientific Center, 123182 Moscow, Russia

R. Osborn

Argonne National Laboratory, U.S.A.

E. S. Konovalova and Yu. B. Paderno

Institute of Problems in Materials Science, Ukrainian Academy of Sciences, Kiev

B. Rainford

University of Southampton, Great Britain

(Submitted 28 March 1995)

Zh. Éksp. Teor. Fiz. **108**, 1064–1080 (September 1995)

Inelastic neutron scattering experiments have been performed on polycrystalline samples of $\text{Sm}_{1-x}(\text{M})_x\text{B}_6$ with $\text{M} = \text{Ca}, \text{Ba},$ and La , for the purpose of investigating how variation of the valence of the Sm ions affects the spectrum of the magnetic excitations. The measurements were performed on the HET time-of-flight spectrometer (in the ISIS facility at the Rutherford Appleton Laboratory) with initial neutron energies equal to 300 meV and 60 meV in the 12–300 K temperature range, which made it possible to investigate both the high-energy spin-orbit transitions and the unusual soft excitation previously discovered in SmB_6 . It has been found for the spin-orbit transitions that a change in valence only causes a corresponding change in their intensity ratio, while all the experimental parameters of the soft excitation, viz., the energy, intensity, region of existence in momentum space, and their temperature dependence, change. These results suggest that the soft excitation belongs to the spectrum of excitations of a new intermediate-valence ground state and permit advancement of an hypothesis regarding the nature of that state. © 1995 American Institute of Physics.

1. INTRODUCTION

The compound SmB_6 is known as a “classical” intermediate-valence system, which was studied actively from the mid-sixties¹ over the course of the next two decades.² The investigations concentrated on two main features of this compound: the intermediate-valence state of the Sm ion and the narrow energy gap in the spectrum of the electron density of states at the Fermi level. Along with the models of Wigner crystallization³ and single-ion hybridization,⁴ which were proposed in the eighties, a model based on a conception of excitonic instability as the driving force of an electronic phase transition⁵ was proposed comparatively recently to describe the microscopic behavior of this intermediate-valence system. In the last few years, owing to some new experimental data on the dynamics of the lattice and the magnetic moment in SmB_6 , which were obtained using inelastic neutron scattering,^{6–8} the models in Refs. 3 and 5 were further developed in Refs. 9,10 and in Ref. 11 to the point of fundamentally different conceptions of the nature of the ground state of the intermediate-valence samarium ion. The source of disagreement is essentially the problem of the relationship between the electronic shielding and the Coulomb interaction in systems with a low density of free electrons. Kasuya¹⁰ treats the ground state as a Kondo

center in a Kondo insulator, while Kikoin and Mishchenko¹¹ regard it as a homogeneous mixed-valence state. Thus, direct experimental information on the properties of the ground state of the samarium ion would be of great interest for obtaining an adequate model of the phenomenon of intermediate valence for this class of substances.

Inelastic neutron scattering is one of the most powerful tools for investigating intermediate valence on the microscopic level¹² because the energy and momentum transfer scales in a neutron experiment are especially suitable. In particular, the influence of spin and charge fluctuations on the dynamics of the lattice and the magnetic moment can be investigated with the necessary degree of detail. In addition, the development of new pulsed neutron sources has expanded the possibilities of neutron spectroscopy to the investigation of spin-orbit and Coulomb¹³ excitations of the f subshell, permitting the easy identification of different f^n configurations on the basis of characteristic magnetic-dipole spectra. One serious obstacle to the realization of this method in the case of SmB_6 is the strong absorption of thermal neutrons by natural samarium and boron. Isotopically substituted samples which ensure a tolerable level of absorption must therefore be used in the experiments.

The results of the first attempt to measure the magnetic

neutron scattering spectrum of a polycrystalline sample of $^{154}\text{Sm}^{11}\text{B}_6$ were published by Holland-Moritz and Kasaya in 1986 (Ref. 14). They postulated the existence of two peaks of a magnetic nature with energies equal to about 15 and 21 meV at near-helium temperatures.

The first experiments performed with the participation of the authors of the present communication on polycrystalline⁷ and single-crystal^{8,15} samples revealed the main features of the spectrum of magnetic excitations of SmB_6 (with a valence $\nu = 2.54$ under normal conditions), particularly the existence of broad peaks corresponding to intermultiplet transitions for the f^6 ($E \approx 36$ meV) and f^5 ($E \approx 130$ meV) configurations along with the presence of a single narrow (at $T \rightarrow 0$) peak with an energy $E \approx 14$ meV. The latter is strongly “localized” in momentum space in both the amplitude and the direction of the momentum-transfer vector \mathbf{Q} . The differences in the character of the momentum dependence of the intensity for these two types of excitations allowed us to speculate that the “former” single-ion states have a resonant (with a short lifetime) character and that the true ground state of the system has a corresponding low-energy excitation, which represents the spectrum of excitations of the weakly bound sixth electron in the f subshell.¹¹

According to the data from L_{III} x-ray spectroscopy,¹⁶ the partial replacement of Sm by Ba increases the valence of Sm, partial replacement by La decreases the valence, and partial replacement by Ca scarcely alters its value, the crystal-lattice parameter increasing in all cases, but to different degrees. Thus, studies of the series of compounds $\text{Sm}(\text{M})\text{B}_6$, where $\text{M} = \text{Ba}, \text{Ca},$ and La , offer a way to trace the relationship between the features of the spectrum of excitations from the ground state and the valence of the samarium ion, which is important for understanding the nature of the intermediate-valence state.

The present communication presents the results of an investigation of the influence of substitution in the rare-earth sublattice on the parameters of the spectrum of magnetic excitations.

2. SAMPLES AND EXPERIMENTAL CONDITIONS

The ^{154}Sm isotope with 98.6% enrichment and the ^{11}B isotope with 99.4% enrichment were used to obtain polycrystalline samples. Compounds with the formulas $\text{Sm}_{0.5}\text{La}_{0.5}\text{B}_6$, $\text{Sm}_{0.5}\text{Ba}_{0.5}\text{B}_6$, $\text{Sm}_{0.5}\text{Ca}_{0.5}\text{B}_6$ were synthesized in amounts equal to 22 g, 20.5 g, and 10.6 g, respectively. In addition, previously prepared samples of SmB_6 (13.5 g) and LaB_6 (9.8 g) were used in the measurements.⁷ X-ray powder diffraction analysis of all the samples obtained confirmed their single-phase state. The slight broadening of the reflections for the sample with barium should be noted. The values of the cubic crystal-lattice parameter (a) for all the compounds investigated are presented in Table I. The values of the valence (ν) of samarium as a function of the composition are also given in that table.

The measurements were performed on the HET time-of-flight spectrometer operating in the ISIS pulsed neutron source (Rutherford Appleton Laboratory) which the energies of the monochromatic neutrons incident on the sample equal 60 and 300 meV. The detection system consisted of five

TABLE I. Lattice parameters a and valence ν according to L_{III} -spectroscopic data determined at $T = 300$ K, as well as the transmission P measured when the energy of the neutrons impinging on the sample equals 300 and 60 meV.

Sample	SmB_6	LaB_6	$\text{Sm}_{0.5}\text{La}_{0.5}\text{B}_6$	$\text{Sm}_{0.5}\text{Ba}_{0.5}\text{B}_6$	$\text{Sm}_{0.5}\text{Ca}_{0.5}\text{B}_6$
$a, \text{\AA}$	4.132(1)	4.156(1)	4.151(1)	4.195(1)	4.139(1)
ν	2.54*	...	2.4**	2.70*	2.55**
$P, \%$					
(300 meV)	79	88	77	81	88
$P, \%$					
(60 meV)	50	82	52	63	68

*Data for our samples.

**Data from Ref. 16.

groups of detectors with mean scattering angles equal to $5^\circ, 10.5^\circ, 16^\circ, 21.5^\circ,$ and 26° , and another group situated at a 136° angle.

The samples were placed in a flat container made from a thin aluminum foil with the dimensions $45 \times 45 \text{ mm}^2$, which are slightly smaller than the effective cross section of the neutron beam. The transmission (P) of the samples in the container is listed in Table I.

The measurements were performed in the 5–300 K temperature range using a closed-cycle refrigerator and a helium cryostat. The typical time of the measurements was 10–20 h with a proton beam current of up to $130 \mu\text{A}$. The contribution to the background due to scattering in the vicinity of the sample was determined from measurements of the empty container. All the necessary corrections were made to the experimental spectra, including normalization to the solid angle of the detection system and the intensity of the incident stream of neutrons, and a vanadium standard was used to absolutize the intensity. The results of the measurements were represented in the form of a scattering law $S_\varphi(Q, E)$, where φ is the scattering angle, Q is the momentum transfer, and E is the energy loss from a neutron upon scattering. The absolutization error is estimated as 20%. The spectra of LaB_6 were used to subtract the phonon contribution to the scattering law⁷ and to obtain the dynamic magnetic response $S_m(Q, E, T)$, which can be represented in the case of paramagnetic neutron scattering in the form

$$S_m(Q, E, T) \propto \chi_{\text{st}}(0, 0, T) \frac{E}{\exp(-E/kT)} F^2(Q) P(E, T), \quad (1)$$

where $\chi_{\text{st}}(0, 0, T)$ is the static magnetic susceptibility, $F(Q)$ is the magnetic form factor, and $P(E, T)$ is the normalized spectral function.

An initial neutron energy $E_0 = 300$ meV was chosen for the measurements of the intermultiplet transitions as the optimal value from the standpoint of combining the range of momentum transfers and the instrumental resolution ($\Delta E_0 \approx 10$ meV). Importance is also attached to the absence of specific nonmonotonicity in the transmission for the samarium sample in the range of energy transfers of interest to us ($E \leq 150$ meV) under these conditions, which facilitates the quantitative treatment of the results. Here it should be borne in mind that the difference between the transmission of

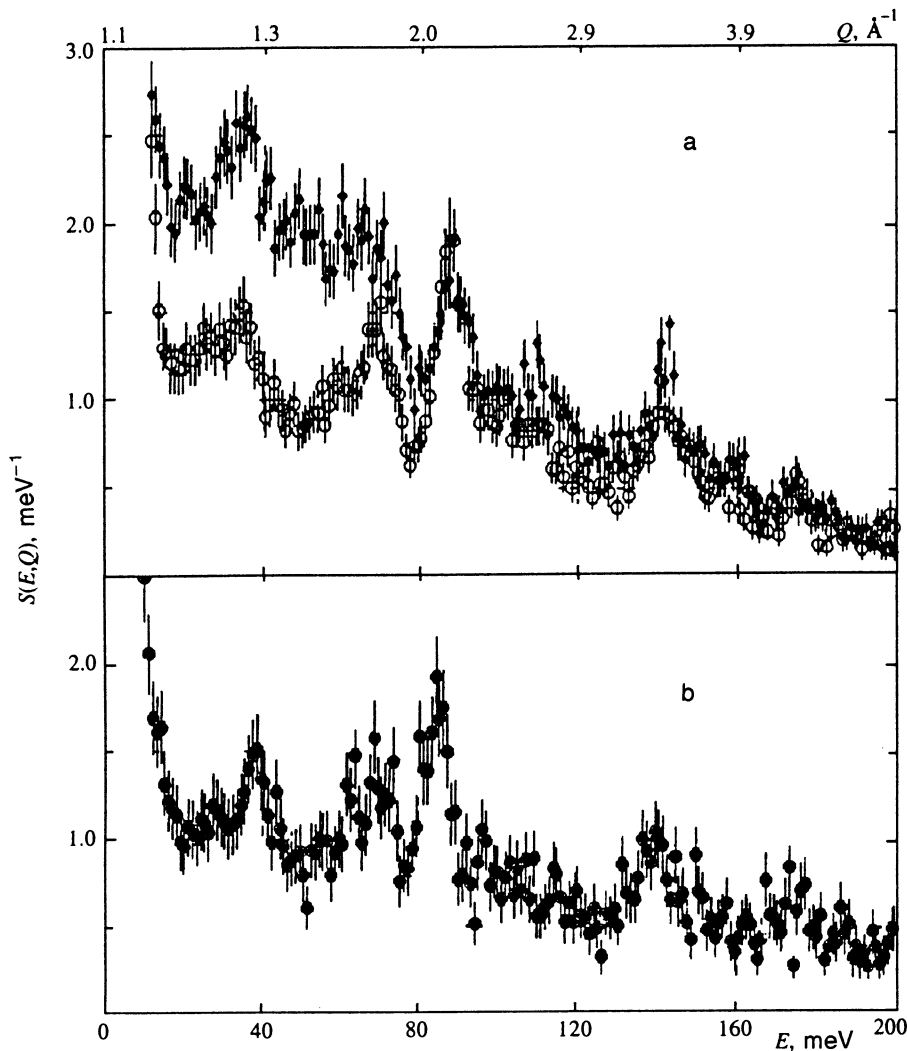


FIG. 1. Total and phonon components in inelastic neutron scattering spectra ($T=20$ K, $\varphi=5^\circ$, $E_0=300$ meV). a) SmB_6 : \bullet —experiment; \circ —phonon component simulated on the basis of the spectra of LaB_6 (see text). b) LaB_6 : experimental spectrum.

SmB_6 and that of LaB_6 , which influences the contribution of multiple scattering for the samarium sample, can lead to some overestimation of the phonon contribution to the scattering at small angles under the procedure employed.

The low-energy part of the spectrum was measured with an initial neutron energy $E_0=60$ meV ($\Delta E_0=1.3$ meV), which is close to the optimal value for minimizing momentum transfer at $E \approx 14$ meV. The use of lower initial energies (down to 30 meV) proved to be ineffective, despite the improvement in resolution, due to the decrease in the illuminating power and the increase in the minimal momentum transfer.

3. RESULTS

3.1. Intermultiplet (spin-orbit) transitions

The energy spectra were measured with an initial neutron energy $E_0=300$ meV for all the samples under identical conditions at a temperature of about 20 K, and the spectrum of the SmB_6 sample was also measured at 300 K.

As an example, Fig. 1 presents plots of $S(Q, E)$ corresponding to $\varphi=5^\circ$ for SmB_6 and LaB_6 . Figure 1a presents a calculated spectrum, which simulates the phonon contribu-

tion to $S(Q, E)$ for SmB_6 . It was obtained by the procedure in Ref. 17, which is based on the assumption of similarity between functionals of the type

$$R(\varphi_1, \varphi_2, E, T) = S_{\varphi_1}(Q, E, T) / S_{\varphi_2}(Q, E, T),$$

which describe the ratio between the scattering laws $S_{\varphi_i}(Q, E, T)$ measured at the scattering angles φ_1 and φ_2 for samples with identical (having similar energy structures) phonon spectra and neutron characteristics. This assumption can be regarded as a rigorous statement when the contributions of the multiple processes to the scattering law (which are most significant for $E < E_0/2$) are equal, which is far from always realizable in practice. The adequacy of the procedure as applied to real samples of rare-earth intermetallic compounds was tested experimentally in Ref. 17. The phonon spectra are made identically using structural analogs with similar electronic properties and masses of the constituent atoms. In our case the mass difference between samarium and lanthanum is less than 7%. The functional $R(5^\circ, 136^\circ, E, T)$ obtained for the LaB_6 sample was used to calculate the scattering law $S_{136^\circ}(Q, E)$ of SmB_6 , which is determined nearly completely by the phonon component of the scattering owing to neglect of the magnetic contribution

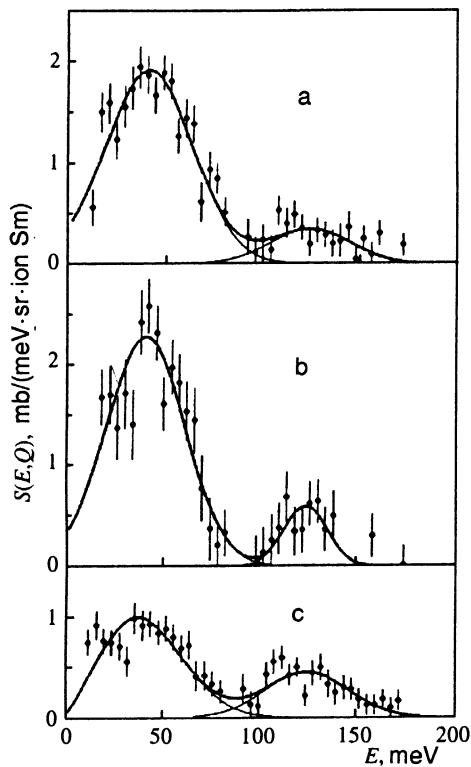


FIG. 2. Magnetic component of the scattering law for SmB_6 (a), $\text{Sm}_{0.5}\text{Ca}_{0.5}\text{B}_6$ (b), and $\text{Sm}_{0.5}\text{Ba}_{0.5}\text{B}_6$ (c) measured with an initial neutron energy $E_0 = 300$ meV and approximated by two inelastic peaks; $\varphi = 5^\circ$.

for $Q > 10\text{--}15 \text{ \AA}^{-1}$, at $\varphi = 5^\circ$. The result is presented in Fig. 1a in the form of the spectrum $S^{\text{ph}}(Q, E)$. The model spectrum $S^{\text{ph}}(Q, E)$ can somewhat overestimate (by $\sim 10\%$) the true value due to the strong absorption of the SmB_6 sample. The difference between $S_{\varphi_i}(Q, E, T)$ and $S^{\text{ph}}(Q, E, T)$ will be regarded below as the magnetic component $S_m(Q, E, T)$ in the spectrum of inelastically scattered neutrons.

Figures 2 and 3 present the magnetic components of the scattering law $S_m(Q, E, T)$ for all the samples investigated, which correspond to excitation only from the lowest state, since the temperature of the samples was sufficiently low (10–20 K) to rule out thermal populating of the excited states.

All the samples exhibit two broad peaks in the spectra near the energy transfers $E \approx 40$ meV and 120 meV. The peaks are appreciably wider greater than the resolution of the spectrometer. The peak near 40 meV is always more intense, but its relative intensity depends on the composition. In particular, it is appreciably weaker in the sample with barium. The magnetic nature of the peaks observed is clearly manifested in the angular dependence of their intensity, which is shown for $\text{Sm}_{0.5}\text{La}_{0.5}\text{B}_6$ as an example (see Fig. 3). An increase in the scattering angle and, accordingly, in the momentum transfer is accompanied by a decrease in intensity. The spectrum for this sample (at $\varphi = 5^\circ$) is distinguished from the spectra in Fig. 2 by the presence of additional structure on the low-energy peak. It can be described as a combination of a broad peak similar to the peak observed for all

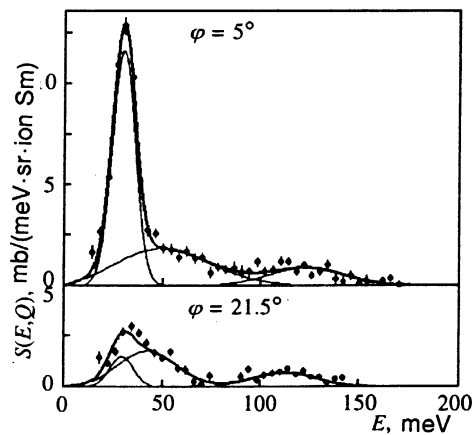


FIG. 3. Magnetic component of the scattering law for $\text{Sm}_{0.5}\text{La}_{0.5}\text{B}_6$ at two scattering angles ($\varphi = 5^\circ$ and 21.5° , $E_0 = 300$ meV, $T = 12$ K). The 21.5° scattering angle corresponds to a large momentum transfer, which results in reduction of the intensity of the peaks.

the other samples at $E \approx 40$ meV, and a comparatively narrow peak of dominant intensity at an energy of about 28 meV. The intensity of this peak decreases with increasing angle somewhat more rapidly than that of the peaks at 40 and 120 meV. The ratio of the integrated intensities of the 40- and 120-meV peaks varies in favor of the high-energy peak as the mean valence increases ($\text{Sm}_{0.5}\text{Ba}_{0.5}\text{B}_6$) and, conversely, in favor of the low-energy peak with the complex structure as it decreases ($\text{Sm}_{0.5}\text{La}_{0.5}\text{B}_6$). The temperature dependence of the spectra can be evaluated from the data obtained for the SmB_6 sample at $T = 300$ K: it was found that the scattering intensity decreases appreciably only for the peak near 40 meV.

Figures 1–3 do not contain points for values of E smaller than 15 meV. This is attributed to the influence of the wings of the elastic scattering peak on the spectrum of the inelastically scattered neutrons, which hampers the reliable isolation of the magnetic component $S_m(Q, E, T)$ in this region. The measurements in this part of the spectrum were performed using neutrons incident on the sample with energy $E_0 = 60$ meV.

3.2. Low-energy excitation

The nature of the low-energy part of the spectrum of SmB_6 was thoroughly discussed in Refs. 7 and 15. The excitation with an energy of 14 meV discovered in experiments on a polycrystal^{7,14} was found to be very unusual, combining the properties characteristic of single-ion excitations with the properties typical of delocalized states. It is characterized¹⁵ by comparatively weak dispersion and the absence of a systematic dependence of the intensity on the reduced wave vector, and it exhibits strong anisotropy of the inelastic structural factor and anomalously rapid (from the standpoint of f -electron excitations) weakening of the latter with increasing momentum transfer. In addition, the temperature dependence of the intensity and width of the 14-meV peak has a characteristic scale (i.e., a temperature at which drastic variation of the excitation parameters occurs), which is signifi-

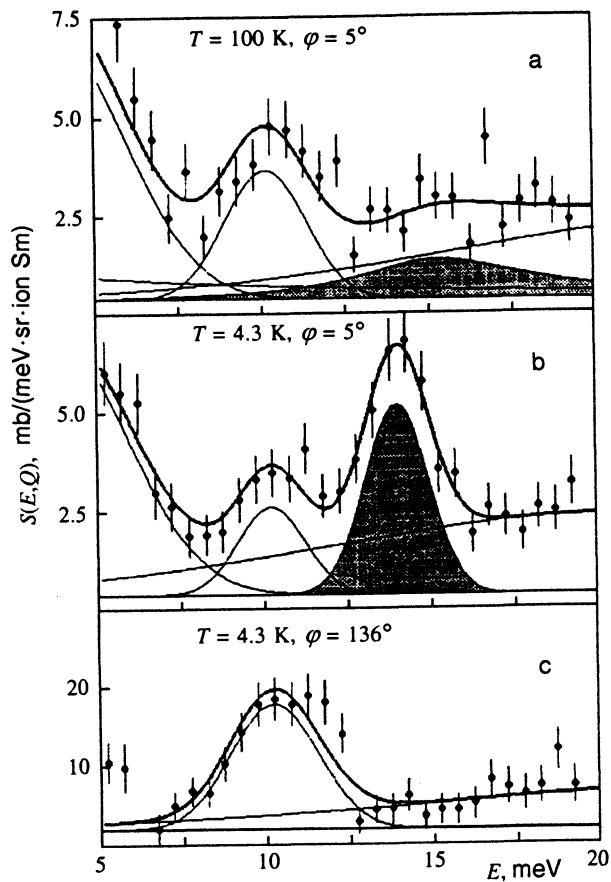


FIG. 4. Low-energy portion of the spectrum for SmB_6 ($E_0=60$ meV). The peak at 10 meV corresponds to the peak of the phonon density of states (c). The peak at 14 meV (shading) exists at a low temperature and a small momentum transfer $Q=0.8 \text{ \AA}^{-1}$ (b). As the temperature rises, the peak broadens, and a quasielastic component appears (a). The slope for small energy transfers at the minimal scattering angle is caused by the contribution from the scattering in structural elements of the crystal.

cantly smaller than the energy of the excitation itself. This is also unusual for single-ion states like crystal-field effects.

The results of the measurements in the low-energy portion of the spectrum for SmB_6 are shown in Fig. 4, and those for the samples with the partial replacement of samarium by calcium, barium, and lanthanum are presented in Figs. 5–7. It is seen that the substitutions in the rare-earth sublattice result in radical alteration of the spectrum: the 14-meV excitation vanishes in all the impurity systems. In addition, a clearly expressed peak with a different, higher energy appears in the case of partial replacement by trivalent lanthanum, but no new separate peaks are observed for the divalent impurities. Figure 4 illustrates a qualitative difference between the peak of the phonon density of states of SmB_6 at $E \approx 10.5$ meV and the electronic excitation at $E \approx 14$ meV. The phonon peak caused by the flat extended section of the dispersion curves in q space for acoustic phonons⁶ follows the known dependence on Q and T for the intensity of lattice excitations, and the 14-meV excitation behaves as a magnetic excitation, i.e., its intensity decreases with both increasing temperature and increasing momentum transfer Q . The

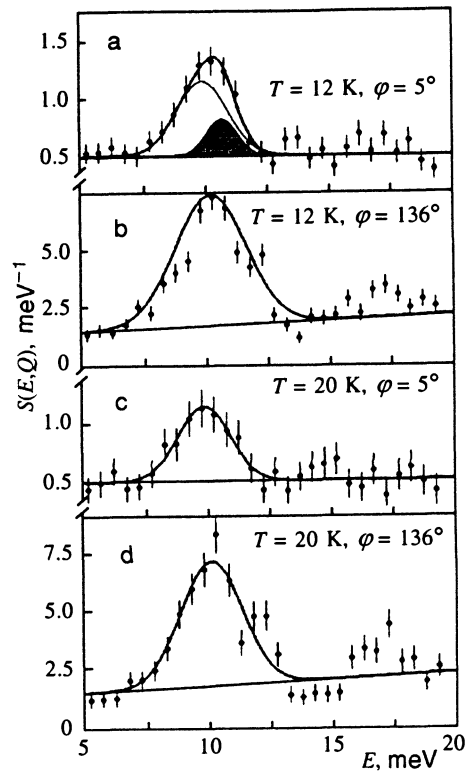


FIG. 5. Low-energy portion of the spectrum for $\text{Sm}_{0.5}\text{Ca}_{0.5}\text{B}_6$ ($E_0=60$ meV). The peak at 10 meV corresponds to the peak of the phonon density of states. An additional peak (shading) with an energy equal to 11 meV appears at the small angle at 12 K.

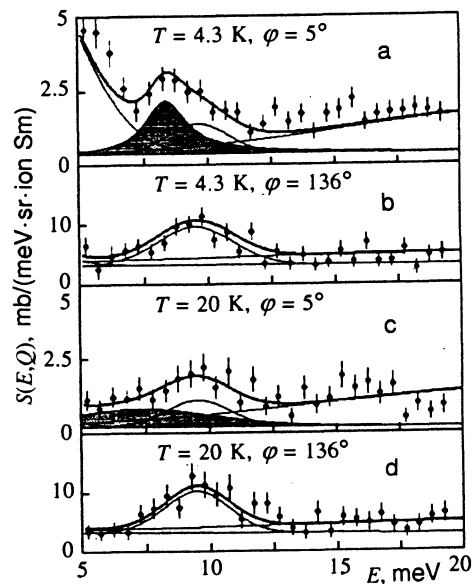


FIG. 6. Low-energy portion of the spectrum for $\text{Sm}_{0.5}\text{Ba}_{0.5}\text{B}_6$ ($E_0=60$ meV). The peak at 9.5 meV corresponds to the peak of the phonon density of states (d), the peak at 8 meV (shading) exists at a low temperature and a small momentum transfer (a) and vanishes when the momentum transfer increases (b) and the temperature rises (c). In the latter case it transforms into quasi-elastic scattering. As in Fig. 4a, the slope at small energy transfers is caused by the contribution from scattering in structural elements of the crystal.

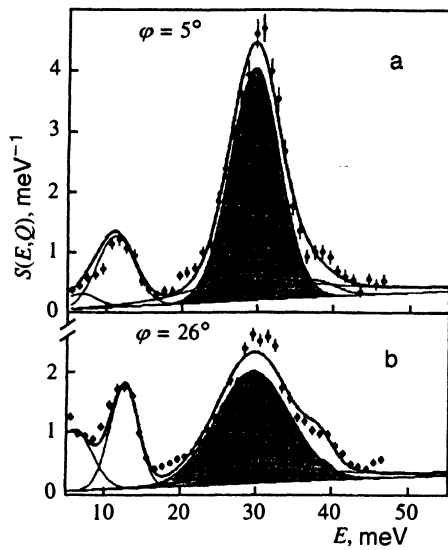


FIG. 7. Low-energy portion of the spectrum for $\text{Sm}_{0.5}\text{La}_{0.5}\text{B}_6$ at two scattering angles ($\varphi = 5^\circ$ and 26° , $E_0 = 60$ meV, $T = 12$ K). The inelastic magnetic scattering in the low-energy region is shaded. The momentum transfers $Q = 1.4 \text{ \AA}^{-1}$ (a) and $Q = 2.5 \text{ \AA}^{-1}$ (b) correspond to an energy of 28 meV.

same magnetic type of behavior is observed for the strong peak with an energy of 28 meV in the spectrum of $\text{Sm}_{0.5}\text{La}_{0.5}\text{B}_6$ (Fig. 7), the energy of the phonon peak remaining practically unchanged ($E \approx 11.0$ meV) relative to SmB_6 .

An analysis of the angular and temperature dependence of the spectra in Figs. 5 and 6 reveals traces of the low-energy excitation in the Ba- and Ca-doped samples. The low-temperature spectra of $\text{Sm}_{0.5}\text{Ca}_{0.5}\text{B}_6$ (Figs. 5a and 5b) for the minimum and maximum scattering angles differ appreciably in the shape of the single observed peak: it is asymmetric, with the maximum displaced toward higher energies at the small scattering angle $\varphi = 5^\circ$. This asymmetry is not associated with the phonon component of the scattering, as is clearly demonstrated by the same spectra measured at a doubled temperature, i.e., at 20 K (Figs. 5c and 5d). The position ($E \approx 10.3$ meV) and shape of the peak at that temperature do not depend on the angle, and the intensity is recalculated from $\varphi = 136^\circ$ to $\varphi = 5^\circ$ by means of a factor coinciding with the ratio between the intensities of the phonon lines for SmB_6 at those angles (compare Figs. 4b and 4c and Figs. 5c and 5d). Increasing the temperature from 12 to 20 K cannot alter the phonon scattering law in the energy range analyzed (~ 10 meV) owing to the negligibly small change in the Bose factor, as is confirmed by a comparison

of the peaks at large angles for these two temperatures (compare Figs. 5b and 5d). It must be assumed that the observed asymmetry at $T = 12$ K is caused by a nonphonon scattering mechanism. The difference between the two contributions is indicated by the fine lines in Fig. 5a: the larger peak corresponds to recalculation of the spectrum in Fig. 5d (or 5b) with the phonon factor, and the smaller peak approximates the experimental excess intensity. It is seen that this excess is described well by a peak with an energy of about 11 meV (the shaded area). Since this additional peak vanishes as the momentum transfer and the temperature increase, it can be attributed to magnetic scattering, i.e., to the appearance of electron excitation.

A similar situation is observed for the sample of $\text{Sm}_{0.5}\text{Ba}_{0.5}\text{B}_6$. The energy of the phonon peak determined from the spectrum for $T = 20$ K and $\varphi = 136^\circ$ (Fig. 6c) is about 10 meV. In the low-temperature spectrum at small angles (Fig. 6a) the maximum of the inelastic peak is clearly displaced in the downward direction (in contrast to the case of $\text{Sm}_{0.5}\text{Ca}_{0.5}\text{B}_6$ considered above) relative to that energy: this shift vanishes both when the temperature is raised and when the scattering angle is increased. Approximation of the corresponding additional contribution by the second peak (the shaded area) gives an excitation energy of about 8 meV. Unlike the cases of partial replacement by Ca and Ba, partial replacement by La (see Fig. 7) results in the appearance of a peak with an energy of about 28 meV, which has a smoother angular dependence than in the case of SmB_6 .

Thus, the partial replacement of samarium by divalent (Ba, Ca) and trivalent (La) elements results in the disappearance of the 14-meV peak in the low-energy portion of the spectrum and the appearance of magnetic features, but with a different energy and a different slope of the angular and temperature dependence. This new peak can be reliably isolated only for the sample with lanthanum. Experimental plots of the dependence of its integrated intensity on the temperature and the momentum transfer are presented in Figs. 8a and 8b. Due to the low intensity, as well as the partial overlap with the phonon peak, we were unable to obtain quantitative characteristics for the low-energy excitations in the other two samples. The qualitative result for these systems is that, as the energy of the excitation decreases, its intensity drops (at least when Q and T are comparable to the corresponding values for SmB_6), and the region for its existence in Q - T space narrows, apparently toward values tending to zero.

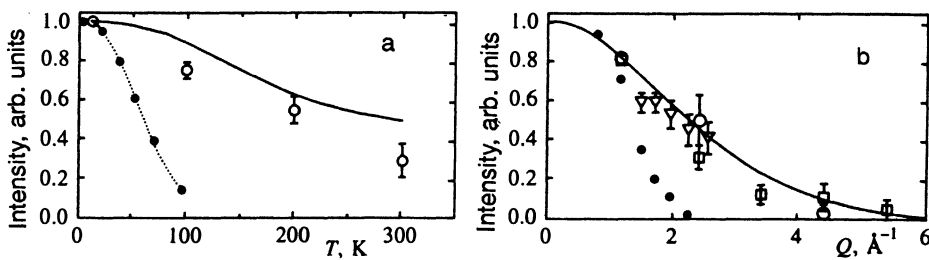


FIG. 8. Dependence of the intensity on the temperature (a) and on the momentum transfer (b) for the 36-meV intermultiplet transition (J^6 configuration, $J = 0 \rightarrow J = 1$) (line), for the 28-meV transition in $\text{Sm}_{0.5}\text{La}_{0.5}\text{B}_6$ (unfilled symbols), and for the 14-meV excitation in SmB_6 [dotted line (a) and filled circles (b)]. Squares and unfilled circles - data obtained with $E_0 = 300$ meV for 12 K and 300 K; triangles - $T = 12$ K, $E_0 = 60$ meV.

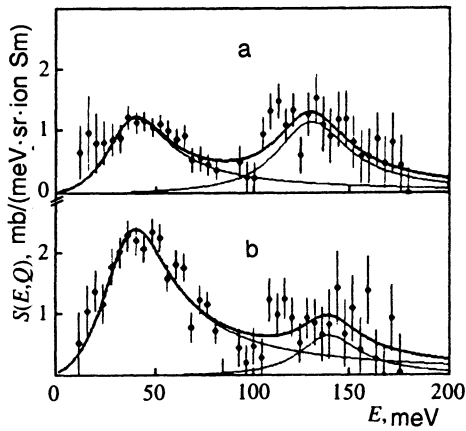


FIG. 9. Spectrum of intermultiplet transitions transformed to zero momentum transfer for samples of $\text{Sm}_{0.5}\text{Ba}_{0.5}\text{B}_6$ (a) and SmB_6 (b); $E_0=300$ meV, $Q=0$, and $T=20$ K.

4. DISCUSSION

The broad peaks observed in the high-energy part of the spectrum of SmB_6 were treated in Ref. 7 as corresponding to excitations of intermultiplet transitions ($\Delta J=1$) for the f^5 (${}^6H_{5/2} \rightarrow {}^6H_{7/2}$, $E \approx 130$ meV) and f^6 (${}^7F_0 \rightarrow {}^7F_1$, $E \approx 36$ meV) parent configurations. This conclusion was drawn on the basis of their intensity ratio and the character of the angular dependence, which corresponded to the calculated inelastic structural factors. If $S_m(Q, E, T)$ is extended to zero momentum transfer and represented in the form $S_m(Q=0, E, T) = S_m(E, T)$, the ratio between their areas directly reflects the ratio between the contributions the parent configurations to the neutron scattering process and can be compared with the results of determining the mean (effective) valence by other methods, particularly L_{III} -edge x-ray absorption spectroscopy. The results of the transformation of the experimental spectra to $Q=0$ for SmB_6 and $\text{Sm}_{0.5}\text{Ba}_{0.5}\text{B}_6$ are presented in Fig. 9. It is seen that the true position of the high-energy peak is shifted closer to 130 meV. This displacement is associated with the great variation of Q over the width of the peak, which causes deformation of the line shape through the form factor. Approximation of the peaks makes it possible to evaluate the ratio between their areas, which agrees well with the mean valence for these two samples, if we utilize the relation

$$\frac{3-v}{v-2} = \frac{S_I(36 \text{ meV})/\sigma_m(J=0 \rightarrow J=1)}{S_I(130 \text{ meV})/\sigma_m(J=5/2 \rightarrow J=7/2)}, \quad (2)$$

where S_I is the measured integrated intensity of the respective peak, σ_m is the cross section of the intermultiplet magnetic-dipole transition, and v is the mean valence.

Partial replacement by lanthanum alters the structure of the 40-meV excitation: its intensity maximum shifts to 28 meV, and it can be regarded, as a whole, as a superposition of the narrow intense 28-meV peak and the former broad peak. For this reason it is difficult to analyze the intensity ratio for the case of $\text{Sm}_{0.5}\text{La}_{0.5}\text{B}_6$. Nevertheless, if the 40-

TABLE II. Positions ε_1 , ε_2 , and widths at half-maximum Γ_1 , Γ_2 obtained using the approximation of the spectral function (1) transformed to $Q=0$ by Lorentzian functions for the experimental spectra of $\text{Sm}(\text{M})\text{B}_6$ samples measured with $E_0=300$ meV.

Sample	SmB_6	$\text{Sm}_{0.5}\text{La}_{0.5}\text{B}_6$	$\text{Sm}_{0.5}\text{Ba}_{0.5}\text{B}_6$	$\text{Sm}_{0.5}\text{Ca}_{0.5}\text{B}_6$
ε_1 , meV	35 ± 1	36 ± 4	35 ± 2	39 ± 2
ε_2 , meV	137 ± 4	116 ± 6	128 ± 3	128 ± 2
Γ_1 , meV	40 ± 9	41 ± 7	38 ± 11	28 ± 9
Γ_2 , meV	43 ± 26	42 ± 20	47 ± 23	26 ± 20

meV excitation is considered as a whole, the ratio of its intensity to the intensity of the 130-meV excitation corresponds to the mean valence of this system.

The results of determining of the energy position and width of the two inelastic peaks present in the spectra of all the samples using the approximation $S_m(Q=0, E, T)$, which is transformed to $Q=0$ using the form factors for the $J=0 \rightarrow J=1$ and $J=5/2 \rightarrow J=7/2$ transitions in Ref. 7 and the analytical spectral function in Ref. 18 are presented in Table 2. In addition, Lorentzian functions were used for $P(E, T)$ in (1). It is seen from Table 2 that the energy and width for these magnetic excitations does not depend on the composition of the sample to within the experimental accuracy.

The influence of the temperature on the intensity of the intermultiplet transitions can be analyzed for SmB_6 . The measurements were performed at two temperatures, 20 and 300 K. It is seen that this temperature difference is not significant for the transition with $E \approx 130$ meV, owing to the small variation of the population of the upper state, which is determined by the parameter $\exp(-E/kT)$, whose value is close to zero. At the same time, for the 36-meV transition an increase in the temperature from 20 to 300 K should have an appreciable influence on the intensity due to the populating of the upper triplet state. The results of an analysis of the influence of the temperature on the experimentally measured area under the 36-meV peak are presented in Fig. 10. The experimental value agrees well with the calculation in the single-ion approximation, and consideration of the weak temperature dependence of the valence¹⁹ improves the agree-

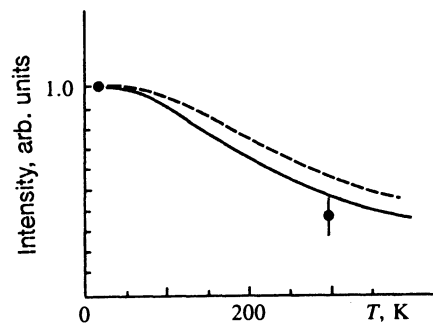


FIG. 10. Temperature dependence of the intensity of the ${}^7F_0 \rightarrow {}^7F_1$ transition (the f^6 configuration). Points – experiment for SmB_6 ; solid line – calculation with consideration of the variation of the valence; dashed line – calculation for a constant valence of samarium.

ment. The intensity of the other peak (at 130 meV) does not depend on the temperature to within the experimental accuracy.

Thus, it can be asserted that the high-energy excitations assigned to the intermultiplet transitions can be described as excitations of the corresponding configurations of the f subshell of the samarium ion, which are represented in the spectra with a weight determined by the mean value of the valence. The qualitative difference from the case of a "mechanical" mixture of two types of ions, viz., Sm^{2+} and Sm^{3+} , is confined to the strong broadening of these excitations, which is associated, as was previously shown for SmB_6 , with a finite lifetime of the quantum-chemical states on the order of 3×10^{-13} s.

The transformation of the spectrum of $\text{Sm}_{0.5}\text{La}_{0.5}\text{B}_6$ illustrates graphically that at low energies the spectrum is very sensitive to the partial replacement of samarium and to the corresponding change in valence. This finding is also an important argument against identification of the observed peaks as transitions between crystal-field-split levels. The opposite character of the changes in the energy position of the peaks and other parameters in the cases of partial replacement by Ba and La is evidence that the change in valence, rather than the presence of defects in the sublattice, is the main driving force of the restructuring of the spectrum. In addition, the results of the measurements performed on a single crystal in Ref. 15, which revealed comparatively weak dispersion of the energy of the peak, imply that the new ground state is a single-ion state to a considerable extent, i.e., the excitations are localized on nearest neighbors and the interaction with other intermediate-valence centers acts as a small correction. The small energy width (in contrast to the case of the intermultiplet transitions) is also evidence in favor of the assignment of this excitation to the spectrum of the ground state. Actually, its width in SmB_6 is restricted by the resolution of the spectrometer, and the width for $\text{Sm}_{0.5}\text{La}_{0.5}\text{B}_6$ amounts to only 7 meV at 12 K. The latter finding is most probably due to an inhomogeneous broadening mechanism, i.e., to the influence of the second coordination sphere, where different combinations of the distribution of La and Sm among the six rare-earth sites are possible, and once again shows that, although the intercenter interaction in the rare-earth sublattice influences the spectrum of excitations, this influence is small. Thus, the main feature of the low-energy excitation is the fact that not only the intensity, but also the energy and the form factor (see Fig. 8) (in contrast to the case of the intermultiplet transitions) are functions of the mean valence. Figure 11 shows the position of the low-energy peak as a function of the mean valence of samarium in the systems investigated. It is seen that the excitation energy correlates with the valence and that the limiting value at $v=2.0$ tends to a value close to the energy of the multiplet transition, i.e., ≈ 36 meV. On the opposite side it tends to zero at $v \geq 2.8$.

Such behavior of the excitation energy as a function of the valence can be understood on the basis of the ideas developed by Kikoin and Mishchenko in Ref. 11. They theorized that the 14-meV excitation in SmB_6 corresponds to a transition with a change in the total angular momentum between the singlet ground state and a triplet excited state of

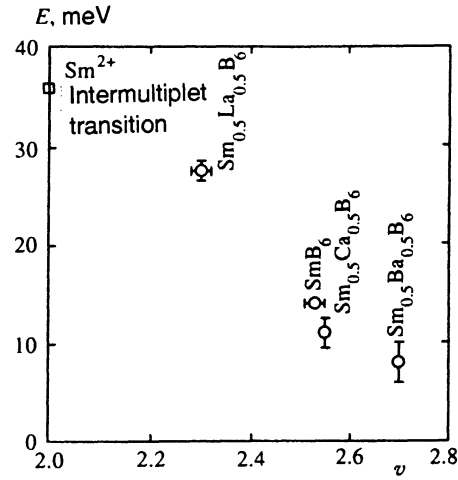


FIG. 11. Dependence of the energy of the "low-energy" excitation on the valence of samarium evaluated for $T = 12$ K for all the samples investigated.

the wave function describing the intermediate-valence state. The wave function of the ground state is

$$\psi_{m,g} = \cos\theta |f_m^6, {}^7F_0\rangle + \sin\theta |f_m^5 B_m^{(f)}, {}^7F_0\rangle, \quad (3)$$

and the wave function for the excited state is

$$\psi_{m,ex} = \cos\theta |f_m^6, {}^7F_1\rangle + \sin\theta |f_m^5 B_m^{(f)}, {}^7F_1\rangle. \quad (4)$$

Here θ is a parameter which characterizes the degree of valence mixing, and $B_m^{(f)}$ describes a combination of electron-hole pairs with suitable symmetry, which makes it possible to construct the 7F_0 state from the f_m^5 subshell and a weakly bound sixth electron distributed between the central position in ion m and its local environment. It follows from the form of (3) and (4) that the transition from the ground state to the excited state is not accompanied by charge transfer, but corresponds to a change in the total angular momentum $J^* = 0 \rightarrow J^* = 1$. The energy of such a transition is determined by the magnitude of the spin-orbit splitting between the initial and final states of the wave functions (3) and (4), i.e., the degree of localization of the electron density described by ψ_m on the central ion. The degree of localization for (3) and (4) is determined by $\cos^2\theta$ and is directly related to the value of the mean valence: for example, for $\theta=0$ we have an f^6 configuration, the valence corresponds to $2+$, and the energy of the transition with $\Delta J^* = 1$ equals 36 meV; as θ increases, the degree of localization decreases, the sixth electron forms a weakly bound state, and the energy of the spin-orbit coupling for ψ_m tends to zero. Thus, according to Ref. 11, after multiplying 36 meV by $\cos^2\theta = 1 - v = 0.46$, we obtain 16 meV, which agrees within the error in the determination of the valence with the value of 14 meV measured for SmB_6 .

It can be postulated that a further increase in the concentration of the trivalent impurities (a shift of the samarium valence toward $2+$) will completely transform the low-energy excitation into the intermultiplet ${}^7F_0 \rightarrow {}^7F_1$ transition. As the concentration of the divalent impurities increases, decreases in the energy, intensity, and size of the region in Q - T space are possible for this excitation with conversion of

the intensity to the quasielastic scattering, which transforms into an excitation resembling an ordinary transition between the crystal-field-split levels for ${}^6H_{5/2}$ as the f^5 configuration is stabilized.

The approach developed in Refs. 9 and 10 does not assume variation of the Kondo temperatures are the ratio between Sm^{2+} and Sm^{3+} changes. Therefore, in this model the low-energy excitations observed in the compounds $\text{Sm}(\text{M})\text{B}_6$ should differ from that proposed for pure SmB_6 .

The behavior revealed by the present and recent¹⁵ investigations in the magnetic neutron scattering spectrum, which is essentially determined by the dynamic magnetic susceptibility, can be used to understand the temperature dependence of the static susceptibility, which is related to the dynamic susceptibility by the Kramers–Kronig relation. The agreement between the temperature of the magnetic susceptibility maximum of SmB_6 (Ref. 19) and the narrow temperature range where the transformation of the low-energy excitation into quasielastic scattering¹⁵ occurs in the neutron spectrum is noteworthy. The region for the existence of the spectrum of magnetic excitations with the singlet ground state corresponds to the low-temperature Van Vleck portion of the susceptibility curve ($T < 40$ K), while the appearance of the quasielastic component and suppression of the 14-meV peak are accompanied by a transition to Curie–Weiss conditions. The adjustment of the spectrum of magnetic excitations observed when samarium is partially replaced by tri- and divalent impurities is also in qualitative agreement with the variation of the character of the susceptibility curves presented in Ref. 19 for $\text{Sm}_{1-x}\text{La}_x\text{B}_6$ and $\text{Sm}_{1-x}\text{Sr}_x\text{B}_6$.

5. CONCLUSIONS

By studying partial replacement of samarium in SmB_6 by di- and trivalent ions we have succeeded in clarifying the relationship between the mean valence of samarium and the parameters of the spectrum of magnetic excitations. The high-energy excitations of the intermultiplet transitions in the short-lived f^5 and f^6 parent states behave as single-ion states, and the mean valence determines the degree to which these excitations are represented in the spectrum. Conversely, all the parameters of the low-energy excitation depend strongly on the mean valence. It can be regarded as a reflection of the properties of the wave function of the true ground state of the intermediate-valence compound in the magnetic spectrum. Here the energy, intensity, and dependence of the excitation on Q are determined by the spatial distribution of the electron density, and the dependence on T characterizes the binding energy of the sixth weakly bound electron to the samarium ion. Thus, if the limiting cases are considered, it can be speculated that no low-energy excitation exists for Sm^{3+} and that the temperature dependence for Sm^{2+} is determined by the energy structure of the unperturbed f subshell of six equivalent electrons.

We note that the model in Refs. 5 and 11, which adequately describes both the lattice and magnetic spectra of excitations of SmB_6 on a single basis, was originally developed to describe the properties, particularly the phonon spectrum, of SmS . Therefore, the existence of a spectrum of magnetic excitations in “golden” SmS with a structure similar to

that for SmB_6 can be postulated. It follows from an analysis of the publications presenting the results of neutron studies of SmS under pressure and of the chemically compressed analog $\text{Sm}_{0.75}\text{Y}_{0.25}\text{S}$ that, although features of the spectrum of magnetic excitations similar to those discovered in the hexaboride were not detected in actual experiments, their existence has not been ruled out in view of the experimental conditions, primarily in the portion of Q – E space investigated. For this reason, a purposeful experiment aimed at finding the low-energy excitation in golden SmS would be very interesting.

In conclusion, we wish to express our sincerest thanks to K. A. Kikoin, A. S. Mishchenko, J.-M. Mignot, and T. Kasuya for numerous fruitful discussions of the physical ideas and experimental results, as well as N. N. Efremova for the valence measurements. We also thank A. Yu. Rummyantsev for his continued interest and active support of this research. P.A.A., V.N.L., and I.P.S. thank the administration of the Rutherford Appleton Laboratory for making it possible to perform the experiments with the unique HET neutron spectrometer.

This research was performed with the financial support of the Russian Fund for Fundamental Research (grant No. 95-02-04734), as well as the International Science Foundation and the Government of the Russian Federation (grant No. M13300).

- ¹É. E. Vainshtein, S. M. Blokhin, and Yu. B. Paderno, *Fiz. Tverd. Tela* (Leningrad) **6**, 2909 (1964) [*Sov. Phys. Solid State* **6**, 2318 (1965)].
- ²P. Wachter, in *Proceedings of the 9th International Symposium on Boron, Borides, and Related Compounds*, edited by H. Werheit, Univ. Duisburg Press, 1987, p. 166; G. Güntherodt, W. A. Thompson, F. Holtzberg, and Z. Fisk, in *Valence Instabilities*, edited by P. Wachter and H. Boppert, North-Holland, Amsterdam, 1982, p. 313.
- ³T. Kasuya, *J. Phys. (Paris)* **37** (Colloq. C4), 261 (1976).
- ⁴R. M. Martin and J. W. Allen, *J. Appl. Phys.* **50**, 7561 (1979).
- ⁵A. S. Mishchenko and K. A. Kikoin, *J. Phys. C* **3**, 5937 (1991).
- ⁶P. A. Alekseev, A. S. Ivanov, B. Dorner *et al.*, *Europhys. Lett.* **10**, 457 (1989).
- ⁷P. A. Alekseev, V. N. Lazukov, R. Osborn *et al.*, *Europhys. Lett.* **23**, 347 (1993).
- ⁸P. A. Alekseev, *Physica B* **186–188**, 365 (1993).
- ⁹T. Kasuya, *Europhys. Lett.* **26**, 277 (1994).
- ¹⁰T. Kasuya, *Europhys. Lett.* **26**, 283 (1994).
- ¹¹K. A. Kikoin and A. S. Mishchenko, *J. Phys.: Condens. Matter* **7**, 307 (1995).
- ¹²M. Loewenhaupt and K. H. Fischer, in *Handbook on the Physics and Chemistry of Rare Earths*, edited by K. A. Gschneidner, Jr. and L. Eyring, 1993, Vol. 16, Chap. 105.
- ¹³R. Osborn, S. W. Lovesey, A. D. Taylor, and E. Balcar, in *Handbook on the Physics and Chemistry of Rare Earths*, edited by K. A. Gschneidner, Jr. and L. Eyring, 1991, Vol. 14, Chap. 93.
- ¹⁴E. Holland-Moritz and M. Kasaya, *Physica B* **136**, 424 (1986).
- ¹⁵P. A. Alekseev, J.-M. Mignot, J. Rossat-Mignod, *et al.*, *J. Phys.: Condens. Matter* **7**, 289 (1995).
- ¹⁶E. S. Konovalova, Yu. V. Paderno, T. Lundström *et al.*, *Poroshk. Metall.* **10**, 78 (1982).
- ¹⁷A. P. Murani, *Phys. Rev. B* **50**, 9882 (1994).
- ¹⁸E. S. Klement'ev, P. A. Alekseev, S. G. Kriventsov, and V. N. Lazukov, Preprint No. IAÉ-5830/9, Kurchatov Institute of Atomic Energy, Russian Academy of Sciences, Moscow, 1994.
- ¹⁹J. M. Tarascon, Y. Isikawa, B. Chevalier *et al.*, *J. Phys. (Paris)* **41**, 1135 (1980).

Translated by P. Shelnitz